Mahasagar-Bulletin of the National Institute of Oceanography, *12*(4), 1979, 201-211.

CONVERGENCE OF EKMAN WIND DRIVEN LAYER AND SURFACE CIRCULATION IN THE ARABIAN SEA DURING SOUTHWEST MONSOON*

J. S. SASTRY AND V. RAMESH BABU

National Institute of Oceanography, Dona Paula-403 004, Goa

ABSTRACT

Using the wind data over the Arabian Sea observed on a typical southwest monsoon day (2nd July, 1963), the vergence and vorticity fields and the net convergence of Ekman wind driven layer at the sea surface have been computed.

Based on Stommel's model, the depth of no meridional motion in the central Arabian Sea has been evaluated and is found to vary from 100 m to 1500 m with corresponding 'σ_t' variation from 24·5 to 27·5. The maximum vertical velocities at the depth of no meridional motion are of the order of -60×10^{-3} cm sec^{-1}. The surface circulation with reference to the evaluated depths of no meridional motion shows alternate bands of meridional flows. The thickness of the surface mixed layer seems to be governed by the field of motion.

INTRODUCTION

Ekman (1905) has divided the oceanic circulation into a shallow wind driven surface layer of frictional influence and a deeper layer of frictionless geostrophic flow. The wind over the sea surface produces a net convergence (or divergence) within the surface layer which leads to the formation of vertical velocity at the bottom of the frictional layer. Under steady conditions, this would be matched at some intermediate depth by the vertical motion resulting from the deep geostrophic meridional flows (Stommel, 1956).

The accuracy of the relative currents largely depend upon the reference level. This level for the Arabian Sea has been arbitrarily fixed by the earlier investigators (Swallow and Bruce, 1966; Düing, 1970; Sastry and D'Souza, 1971 and Rao, Ramesh Babu, Fernandes and Varadachari, 1976). In this paper, the authors present an analysis of the hydrographic data in the Arabian Sea to deduce the level of no meridional motion (Stommel, 1956). Further an attempt has been made to compare the surface circulation patterns derived by the earlier workers with the circulation pattern obtained with reference to the level of no meridional motion.

DATA AND RESULTS OF ANALYSIS

For the present analysis, the wind distribution on a typical monsoon day (2nd July, 1963) is considered. The wind field (Fig. 1) based on the kinematic analysis of Miller and

* Abstract of this paper was presented at the 'Symposium on Environmental modelling of physical oceanographic features as applied to Indian Ocean' held at Naval Physical and Oceanographic Laboratory, Cochin, February 23-24, 1978.

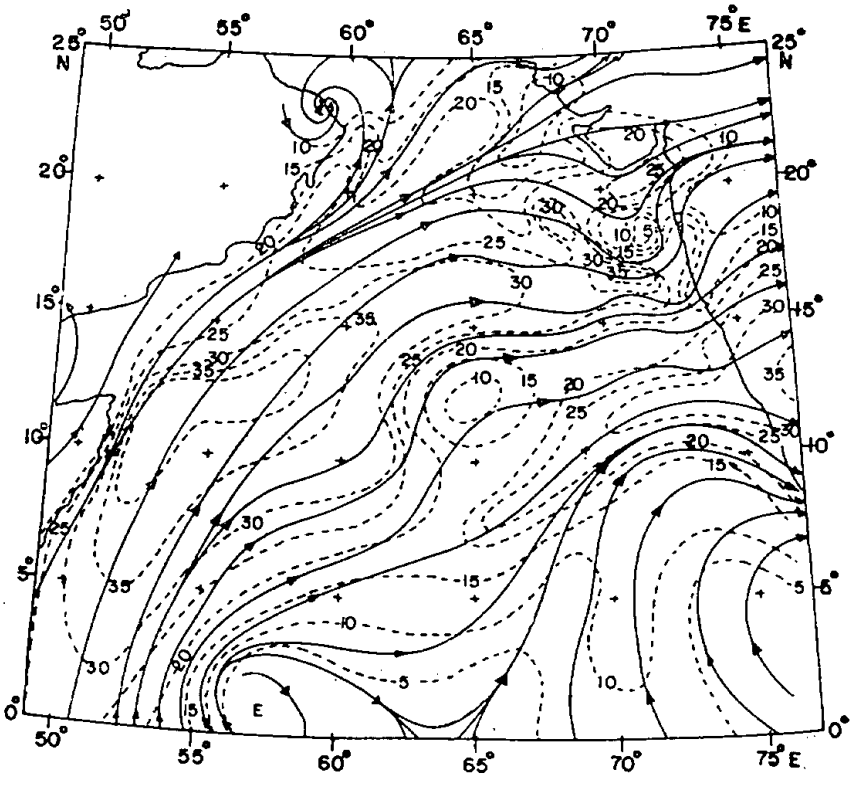

Fig. 1. Kinematic analysis of the surface layer wind for 2 July, 1963 (After Miller & Keshavamurthy, 1968). ——Stream lines -----Isotachs in knots.

Keshavamurthy (1968) forms the basic data for this analysis and this has been chosen since this data set is the only available one coinciding with the period of oceanographic observations (July–August '63). The wind speed and direction were interpolated for 1° squares. This wind was assumed to be statistically steady and vertically homogeneous over the layer (0–900 m).

The wind stress $\vec{T}$ has been computed for each 1° square according to the quadratic equation $\vec{T} = \rho C_D W^2$, where ρ is the density of air, 'C_D' the drag coefficient and 'W' the wind speed. According to Deacon, Sheppard and Webb (1956), C_D has a constant value of 0·0008 in the range of wind speeds 0 to 9 knots, increases linearly to 0·0024 between 9 and 23 knots and then becomes steady for higher wind speeds. Computations of $\vec{T}$ were made using the above C_D values. The density of air is taken as $1{\cdot}2259 \times 10^{-3}$ gm cm^{-3}.

The wind stress divergence (Div $\vec{T}$) is estimated by

$$\text{Div}\,\vec{T} = \frac{\partial T_x}{\partial x} + \frac{\partial T_y}{\partial y}$$

$$= \tfrac{1}{2}\left[\left\{\frac{(T_{x1}+T_{x4})-(T_{x2}+T_{x3})}{\Delta x} + \frac{(T_{y1}+T_{y2})-(T_{y3}+T_{y4})}{\Delta y}\right\}\right]$$

where T_x and T_y represent the zonal and meridional components of the wind stress

respectively. In the finite difference method, subscripts represent the conventional grid numbers around the point of computation with finite interval of $\triangle X$ of 1° longitude and $\triangle Y$ of 1° latitude. The vertical component of relative vorticity ($\text{Curl } \vec{T}$) of the wind stress is computed.

$$\text{Curl } \vec{T} = \frac{\partial T_y}{\partial x} - \frac{\partial T_x}{\partial y}$$

$$= \tfrac{1}{2}\left[\frac{(T_{y1}+T_{y4}) - (T_{y2}+T_{y3})}{\triangle x} - \frac{(T_{x1}+T_{x2}) - (T_{x3}+T_{x4})}{\triangle y} \right]$$

The net convergence (or divergence) at surface of the Ekman wind driven layer, F(0), is given by

$$F(0) = \frac{\partial}{\partial x}(T_y/f) - \frac{\partial}{\partial y}(T_x/f)$$

where f is the coriolis parameter.

A. Wind stress divergence, curl and convergence of Ekman layer

Charts showing the wind stress divergence, relative vorticity and the net convergence of Ekman layer over the Arabian Sea are presented in Figs. 2, 3 and 4.

Fig. 2 shows the maximum value of divergence (> 30×10^{-8} dynes cm^{-3}) around 10°N and 58°E to the east of the region of strongest winds observed (Fig. 1). The divergence

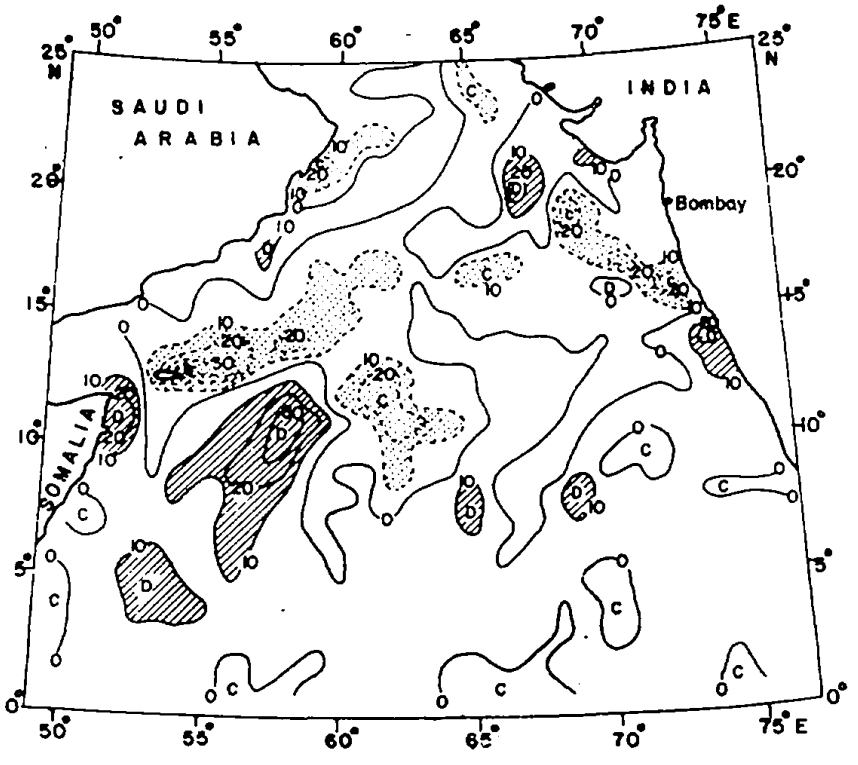

Fig. 2 Vergence field (10^{-8} dynes cm^{-3}). C-Convergence, D-Divergence.

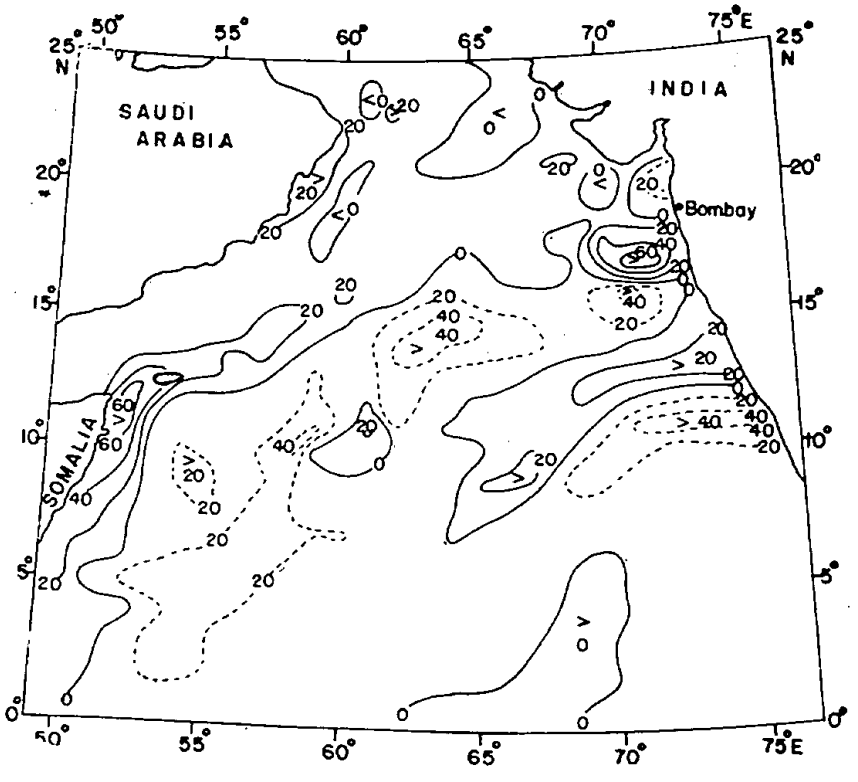

Fig. 3. Surface wind stress curl (10^{-8} dynes cm^{-3}). ----negative values.

attains minimum values towards west before increasing again to moderate values ($>20 \times 10^{-8}$ dynes cm^{-3} off the northern Somalia coast. Near Socotra Island, maximum convergence ($> 40 \times 10^{-8}$ dynes cm^{-3}) is observed and relatively lower values are seen in the central and north eastern portions of the Arabian Sea as well as off the coast of Arabia. A zone of divergence is also observed in an area off the central west coast of India.

The vorticity field (Fig. 3) shows maximum cyclonic curl (of intensity greater than 60×10^{-8} dynes cm^{-3}) off Somalia and Indian coasts (off Bombay). Areas off the central west coast of India and Arabia also experience cyclonic curl but with low intensity ($>20 \times 10^{-8}$ dynes cm^{-3}). The anticyclonic curl is strong ($>40 \times 10^{-8}$ dynes cm^{-3}) in the central as well as in the south western portions of the Arabian Sea and also off the southwest coast of India.

Maximum negative values of F(0) are encountered in the southwest Arabian Sea ($> 60 \times 10^{-3}$ cm sec^{-1}). Off the Kerala coast F(0) has smaller values ($> 10 \times 10^{-3}$ cm sec^{-1}). The divergence in the Ekman layer is found in the areas off the coasts of Somalia and south of Bombay. A zone of divergence in the Ekman layer is situated in a southwest to northeast direction from 65°E to the central west coast of India (Fig. 4).

B. Depth of no meridional motion

According to Stommel (1956),the depth of no meridional motion can be determined by a combination of the usual dynamic method of computation of geostrophic currents

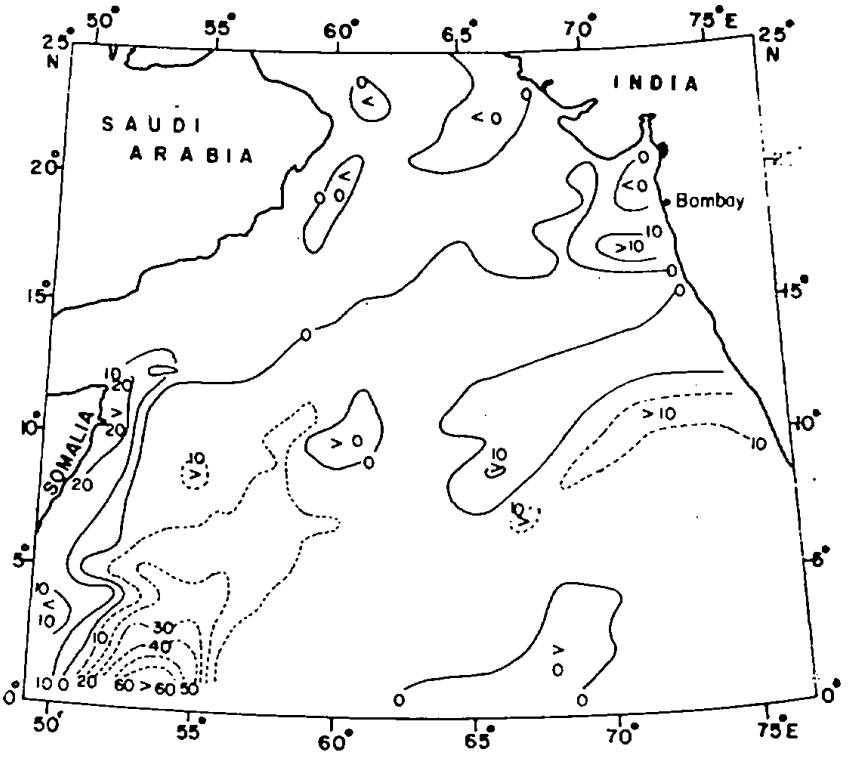

Fig. 4. Net convergence of Ekman wind driven layer F(0) (10^{-3} cm sec^{-1}). ----negative values.

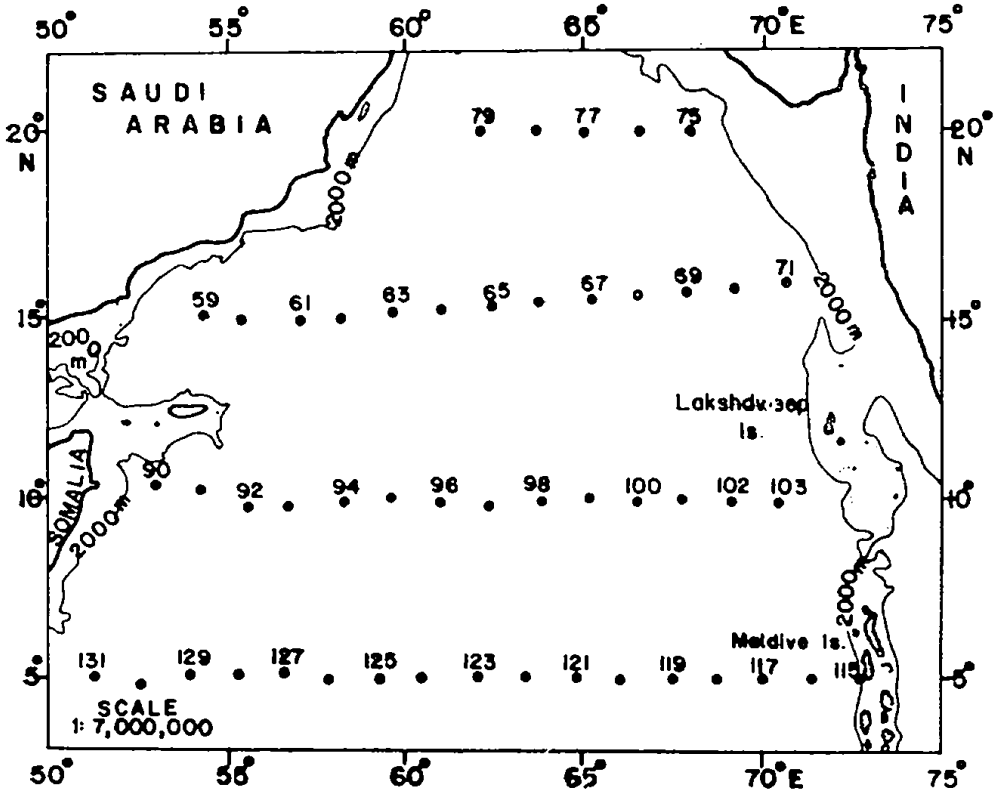

Fig. 5. Station location map.

for a pair of hydrographic stations located on the same latitude and the convergence (or divergence) of the Ekman layer.

According to him

$$\rho v = \phi(z) + C$$

where

v is the meridional component of the current

ρ is the density

$$\phi(z) = -g/f \int_{-B}^{z} \frac{\partial \rho}{\partial x}\, dz$$

g is the acceleration due to gravity

f is the Coriolis parameter

$$C = \frac{1}{B}\left[\frac{f^{F(0)}}{\beta} - \int_{-B}^{0} \phi(z)dz\right]$$

β is the Rossby parameter $(\partial f/\partial y)$

B is the depth to the bottom

In the present study, B is chosen as the depth for which nearest data to the bottom are available.

The vertical profile of 'ρW' is derived from $\rho W + F(Z) = \frac{B}{f}\left[\int_{-B}^{\circ} \phi(Z)dZ + C(Z+B)\right]$

where F(Z) is negligible below the frictional layer. The vertical distribution of $\phi(Z)$ and 'ρW' are evaluated for each pair of hydrographic stations situated on same latitude. In

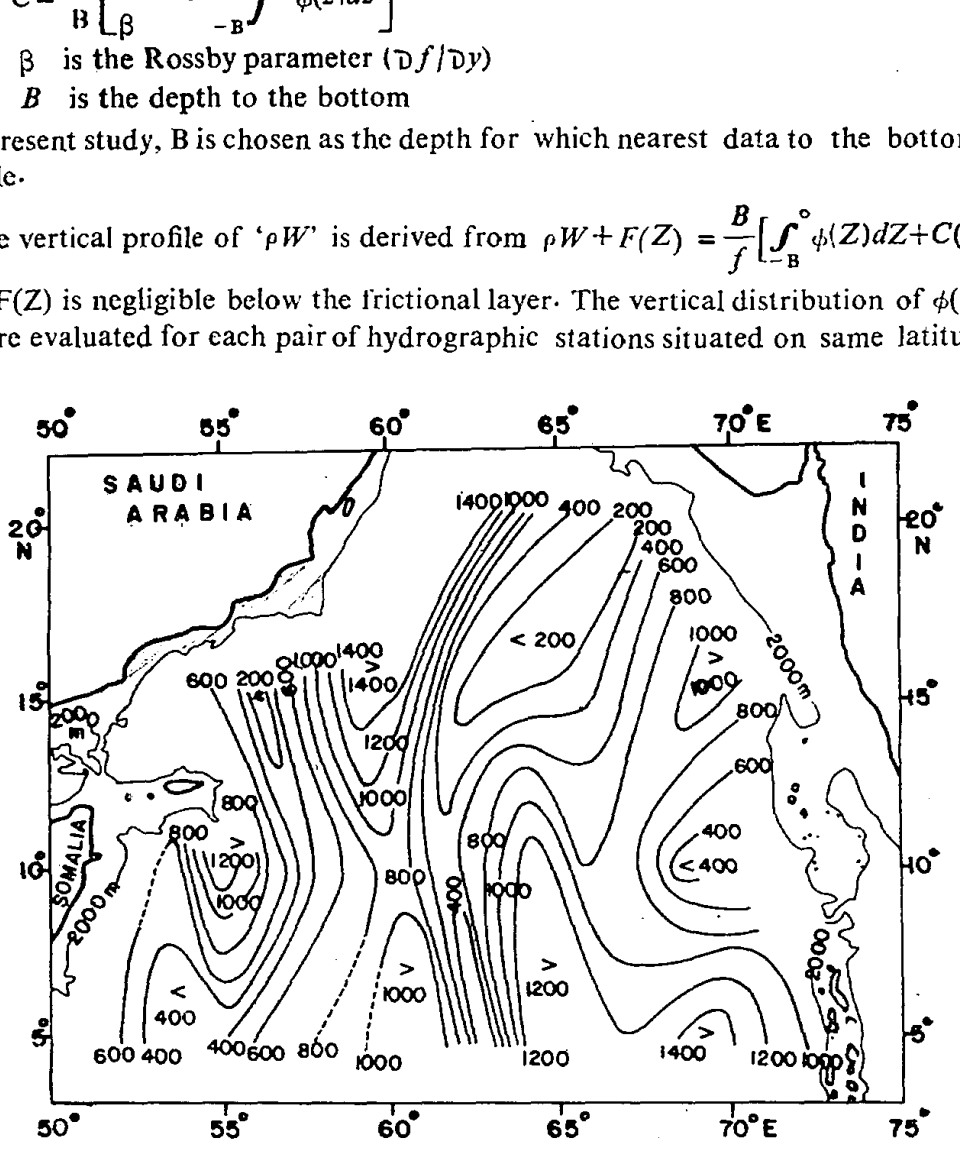

Fig 6. Depth of no meridional motion (metres).

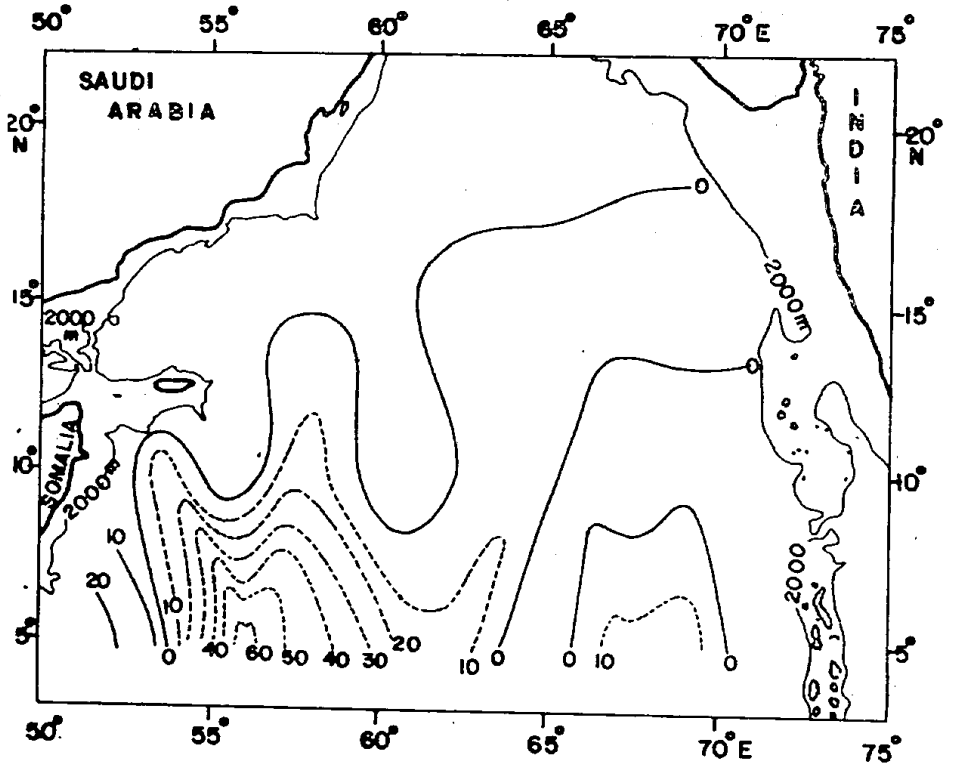

Fig. 7. Maximum vertical velocity 'W' (10^{-3} cm sec^{-1}) evaluated at the depth of no meridional motion. ----negative values.

the present investigation, the station data collected by the US research vessel *Atlantis* during the period of July-August, 1963 have been used and the station locations are shown in Fig. 5. The depth of no meridional motion and the maximum value of 'ρW' found at this depth are plotted for each pair of the stations and their distributions are shown in Figs. 6 & 7. The depth of no meridional motion varies over a wide depth range. A well defined trough exists in the central portions approximately along 60°E and a ridge on its eastern side bounded by 200 m and 400 m depth contours on the north and south respectively. In the eastern Arabian Sea, the topography of this surface indicates a ridge at 10°N and 69°E. On either side of this ridge, the surface slopes to depths greater than 1000 m.

Fig. 7 shows that the vertical velocity is directed upward at the depth of no meridional motion, in the regions off Somalia and north-western Arabian Sea whereas in the south western part, the motion is downwards predominantly. Maximum velocities of the order of 25×10^{-3} cm sec^{-1} were encountered at 5°N about 300 miles from the Somalia coast. An interesting feature is the presence of strong gradient in the areas of downward vertical velocity ($>60 \times 10^{-3}$ cm sec^{-1}) between the stations 127 and 128.

C. Surface circulation

The surface flow pattern relative to the depth of no meridional motion is presented in Fig. 8. The isolines are drawn at intervals of 25 dynamic centimeters. It shows that the circulation basically consists of several clockwise and anticlockwise gyres.

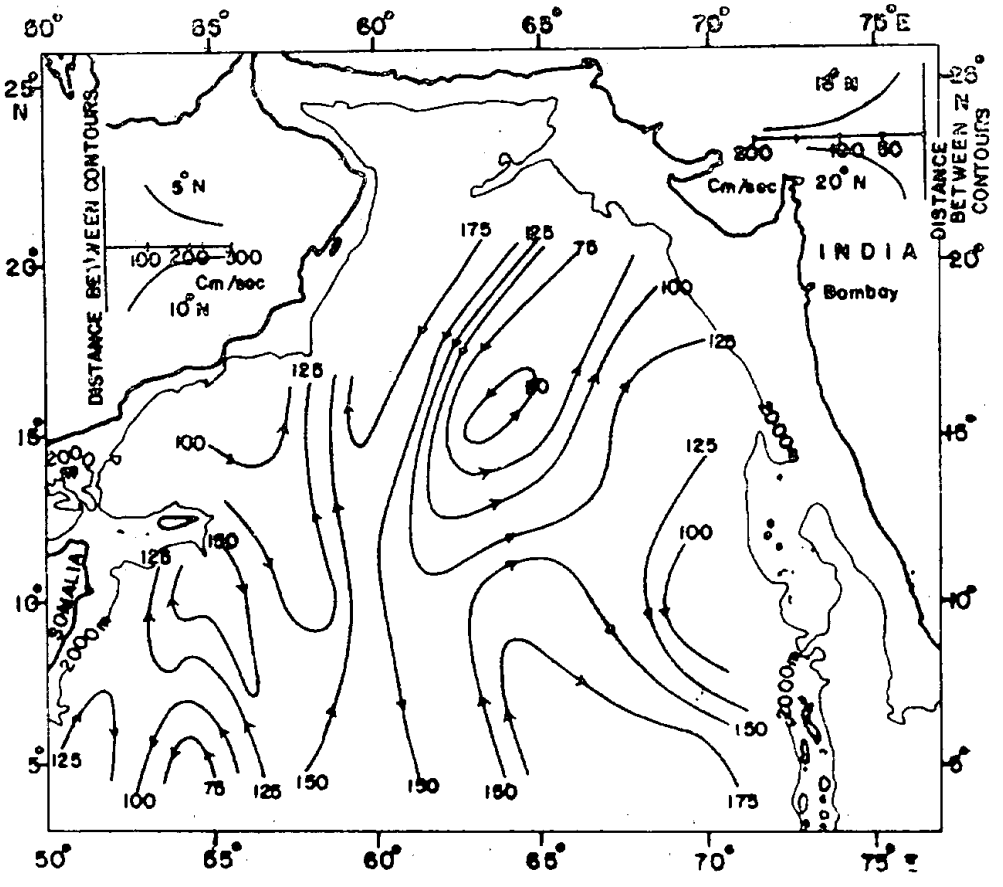

Fig. 8. Dynamic topography of the sea surface (Dynamic cm) relative to the layer of no meridional motion.

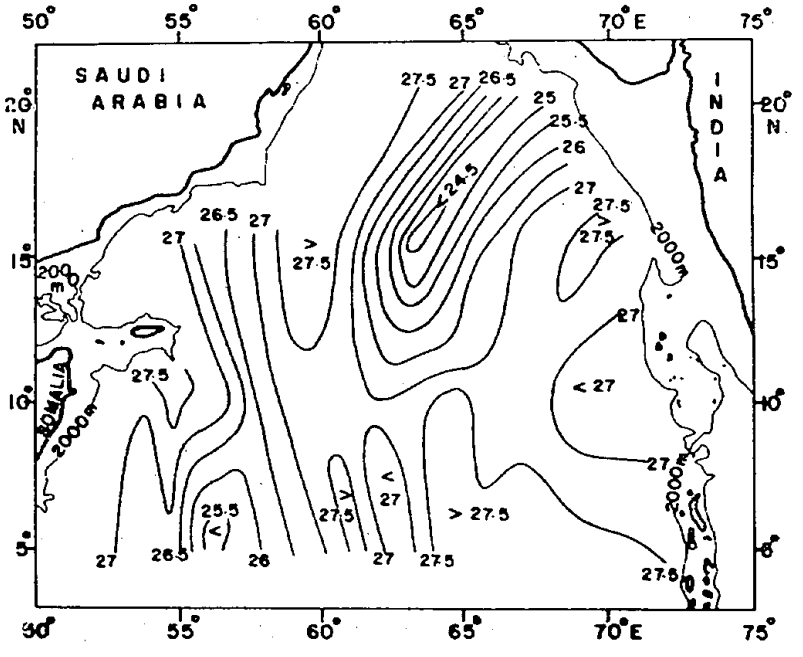

Fig. 9. Density (σ_t) at the depth of no meridional motion

The net flow pattern at the surface could be conveniently divided into two general meridional flows with alternate directions, one moving northward in the region west of 60°E and another moving southward east of it. In the western portion, a clockwise gyre south of Socotra and an anticlockwise gyre further south centered around 5°N and 55°E are clearly seen. The flow in the eastern region consists of two large gyres–one cyclonic and another anticyclonic (north and south of 10°N respectively) merging with the cyclonic circulation near the Lakshadweep Islands. The distribution of 'σ_t' at the surface of no meridional motion shows large variation from 24.5 to 27.5 (Fig. 9).

In order to study the processes which maintain the surface mixed layer, the distribution of vorticity with reference to the β-plane $\left[F(0) \times \frac{f}{\beta}\right]$ is shown in Fig. 10. Maximum values (+ve and –ve) of the order of 12×10^5 cm^2 sec^{-1} are observed at stations 61, 62 and 66; 67, 93 and 94 respectively.

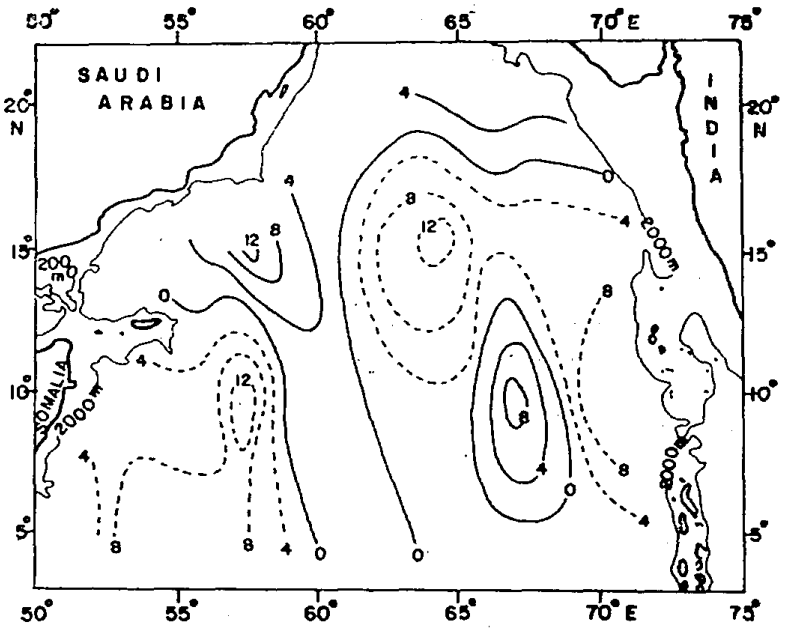

Fig. 10. Distribution of $F(0) \times \frac{f}{\beta}$ (10^5 cm^2 sec^{-1})

When $F(0) \times \frac{f}{\beta}$ values are compared with the distribution of the depth of surface mixed layers (Fig. 11) it is seen that a relation seems to exist between the two in the northern Arabian Sea.

DISCUSSION

The earlier studies on the surface water circulation during the southwest monsoon season, utilizing the same hydrographic data are those of Bruce (1968), Düing (1970) and Sastry and D'Souza (1971). They have used different reference levels fixed arbitrarily and the surface circulation derived by them comprises of several cyclonic and anticyclonic cells over the Arabian Sea. The flow between 5°N and 15°N is found to consist of alternate

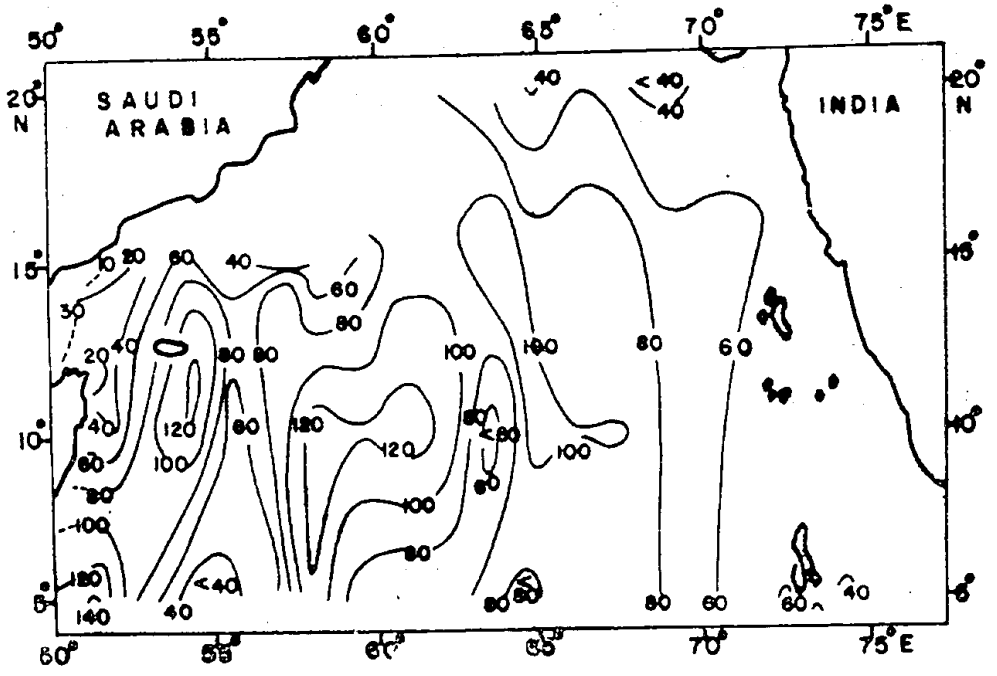

Fig. 11. Thickness of surface layer (metres) (After Sastry & D'Souza, 1970).

meridional flows surrounding these cells. The surface circulation derived in the present study shows features similar to those derived by the above authors in general. For example, the cyclonic circulation around Lakshadweep Islands and the anticyclonic circulation south of Socotra are clearly seen in these studies. The contour interval is 25 dynamic centimeters in Fig. 8 and hence the surface circulation does not appear as complex as given by Düing (1970) and Sastry and D'Souza (1971). The basic difference in the present pattern as compared to that of Düing is the occurrence of a large anticlockwise gyre in the central Arabian Sea.

Sastry and D'Souza (1970) have studied the nature and variation of thickness of the surface mixed layer and concluded that it is related more closely to the surface circulation than with the wind distribution. They point out that the mixed layer (120 m) is well developed in the clockwise gyre than in the anticlockwise gyre (40 m).

Since the circulation, as derived here, is based on the Ekman convergence (or divergence) at the surface and geostrophic flow, it is reasonable to think that convergences and divergences at the surface play a prominent role in the development of surface mixed layer. Keeping in mind that the data on wind stress pertains to a single day and the hydrographic data over a period of two months, these data sets could not be compared for a realistic assessment of the variations on the mixed layer thickness and the wind stress curl. However, it may noted that in the zones of negative curl $\vec{\tau}$, the mixed layer depth is larger compared with those in the zones of positive curl $\vec{\tau}$. Further investigations are needed to establish the relationship.

ACKNOWLEDGEMENTS

The authors wish to express their sincere thanks to Dr. S.Z. Qasim, Director, National Institute of Oceanography, Goa, for his interest. Thanks are also due to Dr. V.V.R.

Varadachari, Deputy Director, NIO for his constant encouragement during this study and to Dr. C.S. Murty for his critical appreciation of this work.

REFERENCES

Bruce, J. G, 1968. Comparison of near surface dynamic topography during the two monsoons in the western Indian ocean. *Deep-Sea Research*, **5**: 665-677.

Deacon, E.L., P.A. Sheppard and E.K. Webb, 1956. Wind profiles over the sea and the drag at the sea surface. *Australian Journal of Physics*, **9**: 511-541.

Düing, W., 1970. *The monsoon regime of the currents in the Indian Ocean.* East-West Centre Press, University of Hawaii. Honolulu, 68 pp.

Ekman, V.W., 1905. On the influence of the earth's rotation on ocean currents. *Arkiv for Mathematik, Astronomi Och Fysik*, **2** : 1-52.

Miller, F.R. and R. V. Keshavamurthy, 1968. *Structure of an Arabian Sea Summer Monsoon System* East-West Centre Press, University of Hawaii, Honolulu, 94 pp.

Rao, L.V.G., V. Ramesh Babu, A.A. Fernandes and V.V.R. Varadachari, 1976. Geostrophic circulation in the northwestern Indian Ocean during the summer Monsoon. *Proceedings of the Symposium on Tropical Monsoons*, Indian Institute of Tropical Meteorology, Poona, p. 218.

Sastry, J.S. and R.S. D'Souza. 1970. Oceanography of the Arabian Sea during the southwest monsoon season Part-I. Thermal structure. *Indian Journal of Meteorology and Geophysics*, **21**: 367-382.

Sastry, J S. and R. S. D'Souza, 1971. Oceanography of the Arabian Sea during the southwest monsoon season Part-II. Stratification and circulation. *Indian Journal of Meteorology and Geophysics*, **22**: 23-34.

Stommel, H., 1956. On the determination of the depth of no meridional motion. *Deep-Sea Research*, **3**: 273-278.

Swallow, J.C. and J. G. Bruce, 1966. Current measurements off the Somalia Coast during southwest monsoon of 1964. *Deep-Sea Research*, **13**: 861-888.